

Heart-Beat Signal Extraction From Phonocardiograms

A. Bouzerdoum, M. A. Tinati*[□]

Edith Cowan University, Perth, WA, Australia

*University of Tabriz, Iran

Abstract: This article introduces a method for constructing a heart-beat signal from a long record of phonocardiogram (PCG). The method comprises a series of algorithms that decompose a long data record of heart sound to its heart-beat cycles using the simultaneously recorded electrocardiogram (ECG). First the cardiac cycles are identified using the synchronized ECG signal. The corresponding heart-beat cycles are then extracted from the PCG signal and used to construct a template signal. Using the correlation of the heart-beat signals with the template signal, the heart-beats corrupted by noise are identified and discarded. The remaining heart-beats are then used to construct a heart-beat signal which is free of artefacts and can be used for various heart sound analysis purposes.

1 INTRODUCTION

A phonocardiogram (PCG) is a recording of an acoustic wave produced by periodical contractions and relaxation of the heart muscles along with acceleration and deceleration of blood within the cardiac structure. The sequence of events occurring during such activities is called the cardiac cycle. Each cardiac cycle is categorized into four basic groups: first, second, third, and fourth heart sounds [1]. Phonocardiograms have been studied for diagnostic purposes for various heart diseases [2]-[5]; and also for better understanding of heart sounds [6]-[8].

The PCG signals are oscillatory in nature; although it may not be exactly periodic in strict mathematical sense. Observation of the evolution of these signals reveals that there are similar events or periods, but they may not exactly reproduce themselves. Furthermore, phonocardiograms are quasi-stationary signals; consequently, their characteristics do not change drastically within few minutes of recordings.

However, analyzing long data records of PCG signals using some signal processing techniques such as time-frequency or wavelet methods imposes a huge computational burden. The heart-beat signal extraction technique presented herein can be used to obtain a single heart-beat signal encapsulating the characteristics of the PCG signal. The extracted heart-beat signal can then be used for analysis or diagnostic purposes.

The proposed heart-beat signal extraction technique is explained in the succeeding two sections. First the electrocardiogram beat cycle detection algorithm is introduced in Section 2. In Section 3, the segmentation of the PCG signal and the reconstruction of a single heart-beat signal are explained. Then in Section 4 experimental results are presented, followed by a concluding remarks in Section 5.

2 HEART-BEAT CYCLE DETECTION

The central idea of the proposed heart-beat separation scheme is the decomposition of phonocardiograms into heart-beat signals through the detection of the heart-beat cycles of the synchronized electrocardiograms; beat cycle detection is easier using ECG signals. In order to accomplish this, first the QRS peaks of the ECG signal are detected, and then the corresponding beat cycles are identified.

2.1 QRS Peak Detection

QRS detection is one of the important tasks in ECG analysis; a great deal of research effort has been devoted to this task [2]. Most of the QRS detectors described in the literature are aimed for analysis of the ECG signal itself. Our aim, however, is to find the temporal location of the peaks of the QRS complexes and use them to separate the heart-beat cycles from the PCG signal. Our QRS detection scheme is divided into two sub-systems: the preprocessor and the decision rule system, as shown in Figure 1. The main concern in the QRS detector is to avoid detection of false peaks, if any.

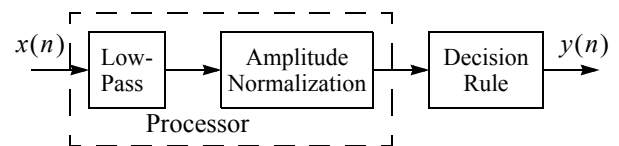


Figure 1 QRS peak detector.

Figure 2 shows the QRS detection algorithm. The input signal, $S_{\text{ecg}}(t)$, is initially normalized in amplitude. This is essential since a thresholding scheme is employed for detection of peaks of the QRS complexes. There are usually some fluctuations in the QRS amplitudes, hence the threshold level is set to a value V_{th} given in Eq. (1).

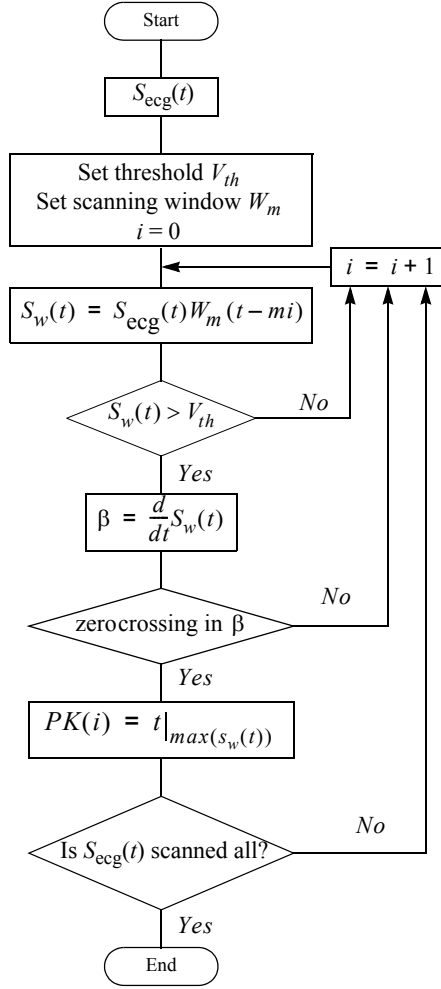
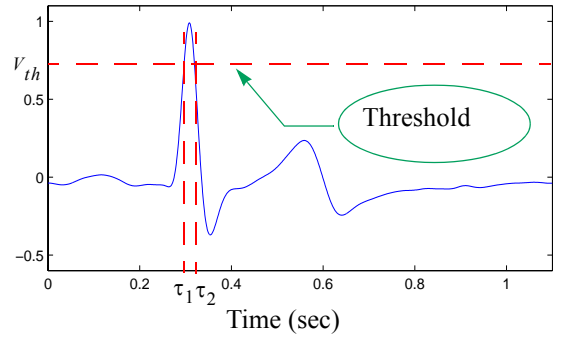


Figure 2 QRS peak detection algorithm.

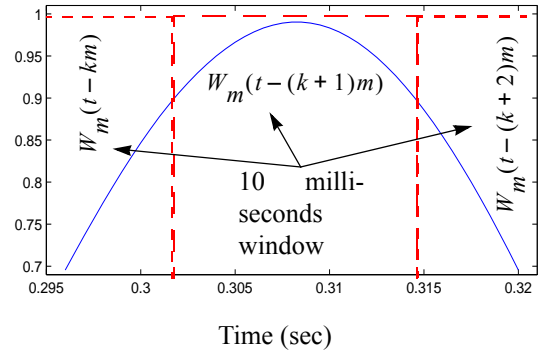
$$0.8 \leq V_{th} \leq 1 \quad (1)$$

The input data is scanned with a rectangular window the width of which is much less than a heart-beat period, whose length could vary from about half a second to more than one second depending on the person. A small window size reduces the possibility of missing any QRS peaks during the scanning process. Within each window the parts of the data that are above threshold are selected and their maximum value is found. The thresholding scheme ensures that only regions of the signal that are in the vicinity of the peak of the QRS complex are considered for peak detection. In Figure 3 shows one cycle of an ECG signal with threshold level V_{th} and a scanning window W_m of length m .

In order to distinguish and locate the position of the actual QRS peak, the slope of the signal above threshold is calculated within each window. Let $W_m(t - mi)$ be the i th window and $S_{ecg}(t)$ be the portion of the QRS



(a) One ECG cycle.



(b) Peak of QRS Complex.

Figure 3 The process of thresholding and windowing the ECG signal.

complex above threshold. The slope of the windowed ECG signal above threshold level is

$$\beta_i(t) = \frac{d}{dt}[S_{ecg}(t)W_m(t - mi)] \quad (2)$$

The zero crossing in $\beta_i(t)$ represents a local maximum in the ECG signal, i.e., a potential QRS peak.

2.2 True QRS Interval Detection

The primary objective of the true QRS interval detection is to ensure that the peaks detected with the algorithm of Figure 2 are real QRS peaks; that is, we want to identify any false detections and remove them. There are two situations in which a false detection may occur: a presence of an artefact whose height is higher than the threshold level, or the presence of small fluctuations (due to noise) near the QRS peak.

The mean interspike (i.e., QRS peak-to-peak) interval is calculated as

$$T = \frac{1}{M-1} \sum_{j=1}^{M-1} PK(j+1) - PK(j) \quad (3)$$

where M is the number of detected QRS peaks, and PK is a vector containing the locations of the QRS peaks. We define the minimum and the maximum acceptable time interval between two consecutive QRS peaks as:

$$\Delta T_{mn} = T - 0.1T \quad (4)$$

$$\Delta T_{mx} = T + 0.1T \quad (5)$$

The average interval between the i th peak and its nearest neighbours is calculated as follows:

$$\delta t_i = \frac{\Delta t_i + \Delta t_{i+1}}{2} \quad (6)$$

where Δt_i and Δt_{i+1} are the time intervals between the i th peak and its preceding and succeeding peaks, respectively; that is,

$$\Delta t_i = PK(i) - PK(i-1) \quad (7)$$

$$\Delta t_{i+1} = PK(i+1) - PK(i) \quad (8)$$

The interval, δt_i , for every detected peak is compared with ΔT_{mn} and ΔT_{mx} . If it is within the interval $[\Delta T_{mn}, \Delta T_{mx}]$, it is accepted as a true QRS peak, otherwise it is considered to be a false peak, and hence rejected. That is, for a true QRS peak, Eq. (9) must be satisfied.

$$\Delta T_{mn} \leq \delta t_i \leq \Delta T_{mx} \quad (9)$$

When a false QRS peak occurs at position i , the value of its average interval δt_i , and possibly those of adjacent peaks, will not satisfy Eq. (9). In particular, there will be a local valley centred on i in the values of the vector δt , the vector whose elements are the intervals δt_i . In order to find the location of the false QRS peak, it is necessary to find the position of the bottom of the valley. This is accomplished by calculating the derivative of the vector δt and finding the position at which the derivative becomes zero. The proposed QRS interval detection algorithm is shown in Figure 4.

2.3 ECG Beat Cycle Detection

In order to detect the beat cycles, the beginning of each cardiac cycle with respect to QRS peaks must be identified. The P-wave is chosen as the beginning of the cardiac cycle. If the time interval between two consecutive QRS peaks is divided into three sections, the P-wave occurs in the third section. The onset of the third section of the i th QRS peak is given by Eq. (10).

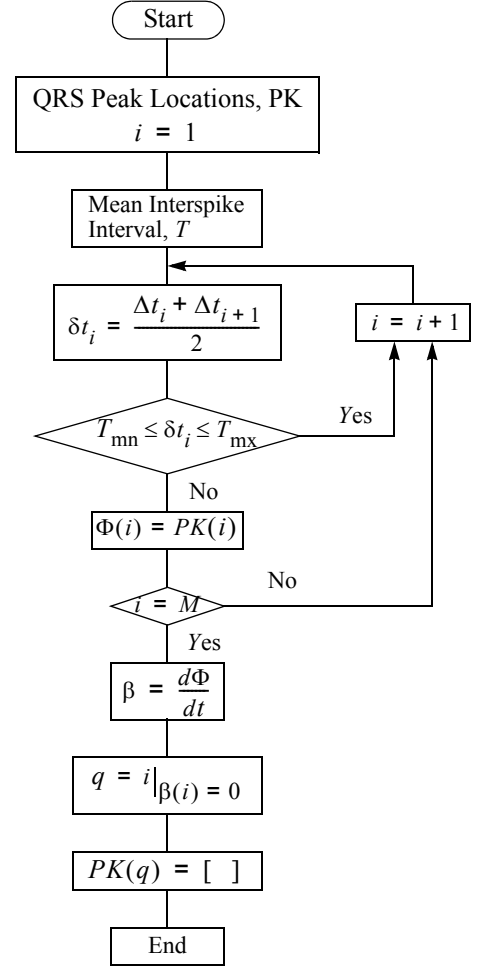


Figure 4 QRS interval detection algorithm.

$$tr_i = PK(i) - \frac{1}{3}[PK(i) - PK(i-1)] \quad (10)$$

where its offset time is the i th entry in the vector PK . This is illustrated in Figure 5.

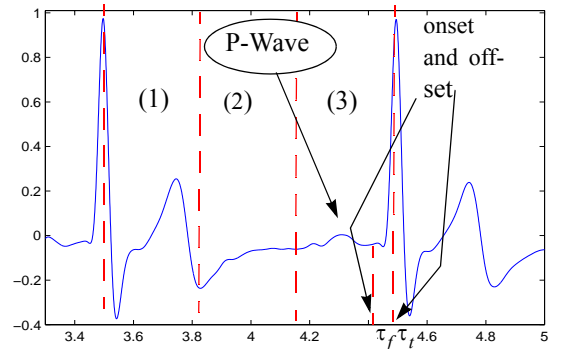


Figure 5 Two consecutive cycles of ECG signal for P-wave recognition.

Since we are going to use the QRS peak detector to find the peaks of the P-waves, it is essential to remove the portion of the QRS complex that falls within section three. This is the part of the signal between τ_f and τ_t in Figure 5. This is accomplished by calculating the slope of the signal from tr_i to PK_i as:

$$mp_i = \frac{d}{dt} S_{\text{ecg}}(t) \quad \text{for } tr_i \leq t \leq PK(i) \quad (11)$$

The signal mp_i is scanned in a bottom-up fashion; that is, scanning starts from the end and proceeds towards the beginning. When the first zero crossing is encountered, the scanning is stopped. This point corresponds to the first minimum in the signal just before the QRS complex. The part of the signal to the right of the zero crossing is discarded. In order to detect the peak of the P-wave, the algorithms of Figure 2 and 4 are applied to the remaining part of the signal. This process is repeated for all detected QRS intervals. The final outcome is a vector the same size as the ECG signal $S_{\text{ecg}}(t)$, the elements of which are all zeros except at the locations of the P-wave peaks, where a value of one is recorded. The flow chart of this algorithm is shown in Figure 6.

3 SEGMENTATION OF PCG SIGNAL

The prime purpose for developing the QRS detection algorithm was to devise a scheme which would enable us to decompose the PCG signal into its beat cycles with minimum error of miss-detection. As was mentioned earlier, the ECG and PCG signals must be recorded simultaneously. Therefore, the decomposition process of the PCG signal into its constituent beat cycles can be accomplished by simply aligning it with the signal obtained by the algorithm of Figure 6, $v_{\text{ecg}}(t)$, which is a train of impulses located at the starts of the cardiac cycles.

3.1 Identification of Artefact-Free Beat Cycles

Among the separated heart-beat cycles, it is necessary to identify and discard those cycles that contain artefacts. Let each PCG heart-beat signal be denoted by $S_{\text{pcg}}^i(t)$, where i is the order of the beat cycle within the PCG signal. A correlation scheme is devised to distinguish the artefact-free heart-beat cycles within the PCG signal. A template signal is constructed for this purpose, and every beat cycle is compared with it. The template signal, $S_{\text{tmp}}(t)$ is constructed by taking the ensemble average of all the beat cycles.

$$S_{\text{tmp}}(t) = \frac{1}{M} \sum_{i=1}^M S_{\text{pcg}}^i(t) \quad (12)$$

where M is the total number of heart-beat cycles.

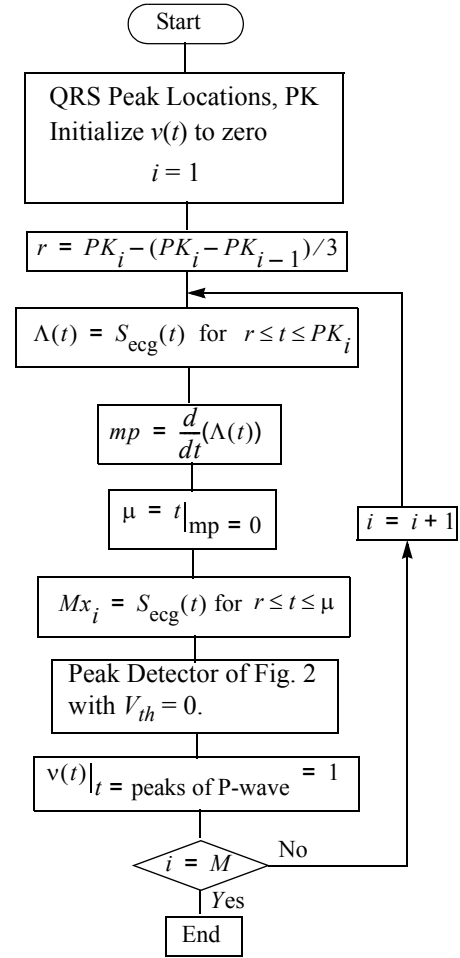


Figure 6 ECG beat cycle detection.

The degree of similarity between the beat cycle waveforms and this template signal is measured by calculating the correlation coefficient of the template signal with each of the beat cycles. The correlation coefficient between the template signal and a given beat cycle is defined as

$$\rho = \frac{C_{\text{tmp, btc}}}{\sqrt{C_{\text{tmp}} \times C_{\text{btc}}}} \quad (13)$$

where $C_{\text{tmp, btc}}$ is the cross-covariance between the template signal and the beat cycles, C_{tmp} and C_{btc} are, respectively, the covariances of the template signal and the beat cycle.

In order to obtain the maximum correlation coefficient possible, the beat cycle is shifted with respect to the template signal. In other words, the correlation coefficient is computed at the smallest time-lag which yields maximum cross-correlation between the two signals.

The cross-correlation of the template signal with the beat cycle is defined as

$$X(\tau) = \sum_{n=0}^N S_{\text{tmp}}(n)S_{\text{btc}}(n-\tau) \quad (14)$$

where N is the length the template signal, which is equal to the length of the beat cycle.

In order to identify the beat cycles corrupted with artefacts, a threshold level for the correlation coefficients is set to 0.9; that is, those beat cycles that have their correlation coefficient below 90% of the maximum correlation coefficient are rejected.

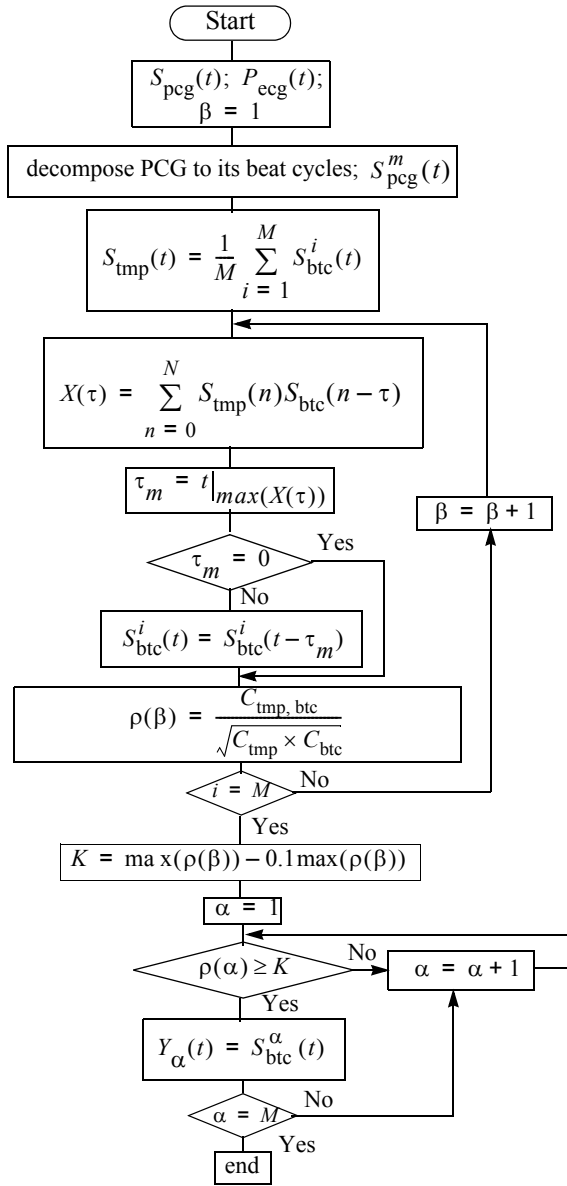


Figure 7 Heart-beat construction algorithm.

3.2 The Heart-beat signal

The final heart-beat signal is reconstructed using only the artefact free beat cycles. The mean signal of the beat cycles is computed in the frequency domain. Frequency domain averaging is used to avoid errors that may occur due to small miss-alignments of the beat cycles in the time domain. To obtain the time domain signal, the averaged frequency domain signal is converted back to the time domain using the inverse discrete Fourier transform (IDFT). The heart-beat cycle reconstruction algorithm is presented in Figure 7.

4 RESULTS

In this section we present the results of applying the algorithms presented in this article to real signals recorded from patients suspected with coronary artery disease. Thirty seconds of synchronously recorded PCG and ECG signals are shown in Figure 8 below; clearly the PCG signal contains some artefacts.

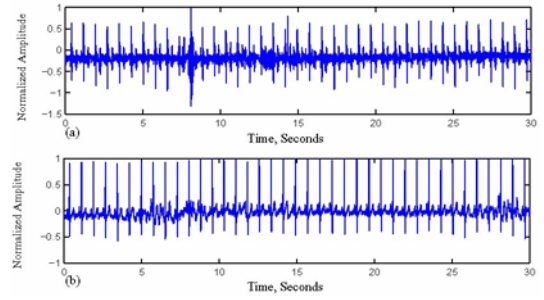


Figure 8 Synchronously recorded PCG (a) and ECG (b) signals.

The ECG signal was scanned with a 10 millisecond long rectangular window. A threshold level of 0.8 was selected, and the QRS detection algorithm was applied. The detected QRS peaks were examined with the algorithm of Figure 4 for false detections. Then the starting points of the cardiac cycles were detected using the ECG beat-cycle detection algorithm (Figure 6). The output of the ECG cycle detection algorithm, the signal $v_{\text{ecg}}(t)$, is shown in Figure 9.

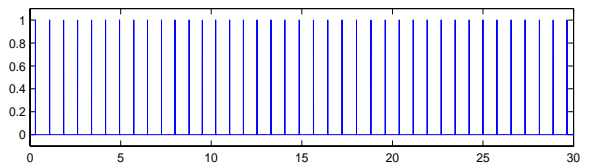


Figure 9 The signal $v_{\text{ecg}}(t)$ obtained from the ECG beat-cycle detection algorithm.

The PCG cardiac cycles were separated by aligning the PCG signal (Figure 8(a)) with the signal $v_{ecg}(t)$ of Figure 9. These extracted PCG cardiac cycles, shown in Figure 10(a), were then used to reconstruct the PCG template signal presented in Figure 10(b).

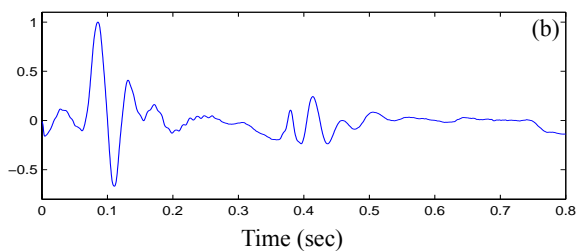
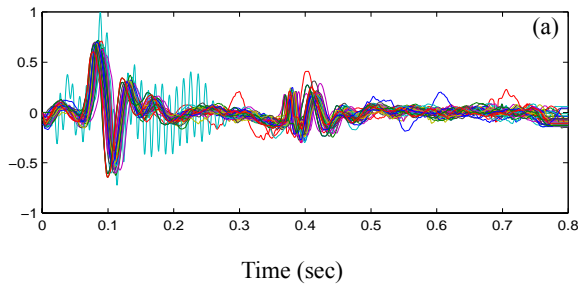


Figure 10 (a) Beat cycles of PCG signal of Figure 8 (a).
(b) PCG template signal.

The correlation coefficients of the template signal of Figure 10(b) with each beat cycle of Figure 10(a) were calculated; the computed correlation coefficients are tabulated below (TABLE 1) and plotted in Figure 11. In Table 1, four correlation coefficients fall below 0.9, but one of them is equal to 0.8946, very close to 0.9. If the threshold level is set at 0.88, as shown in Figure 10, only three beat cycles that have their correlation coefficients below the threshold level, and hence are rejected. Figure 12 illustrates the accepted and rejected PCG beat cycles. The final heart-beat cycle is constructed using only the artefact free beat cycles as described in Section 3.2. The final PCG beat signal is presented in Figure 13. It is an artefact free signal, which represents the typical heart-beat cycle of the person from who the signal was recorded.

TABLE 1 – Correlation coefficients of PCG template signal with individual beat cycles.

0.9660	0.9625	0.9395	0.9505	0.9375
0.9634	0.9482	0.9387	0.9170	0.6944
0.6568	0.9181	0.8946	0.9060	0.8681
0.9194	0.9455	0.9198	0.9322	0.9323
0.9613	0.9400	0.9172	0.9359	0.9490
0.9405	0.9400	0.9278	0.9448	0.9669
0.9645	0.9394	0.9500	0.9389	0.9658
0.9485	0.9386	0.9171		

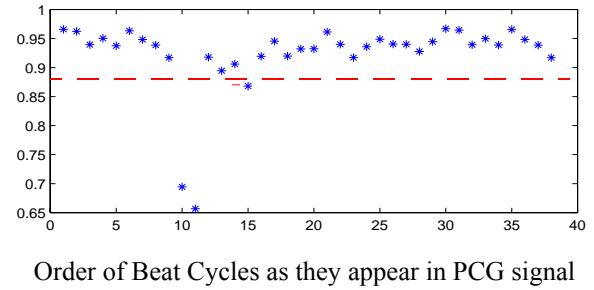


Figure 11 Correlation coefficients for signals of Fig. 10(a) with the template signal of Fig. 10(b).

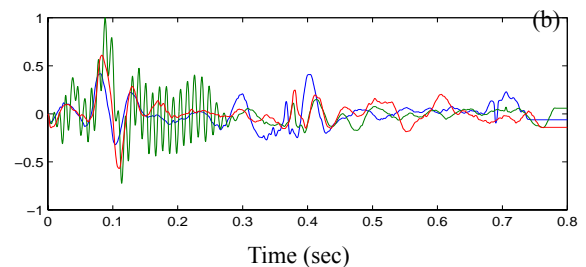
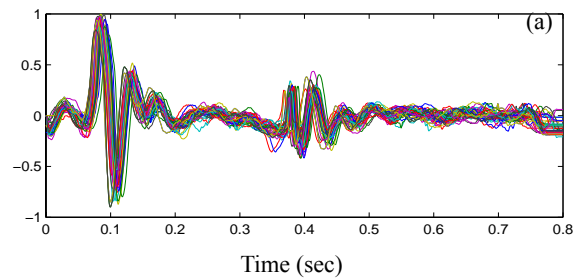


Figure 12 (a) Accepted beat cycles, and (b) rejected beat cycles for PCG signal of Figure 8 (a).

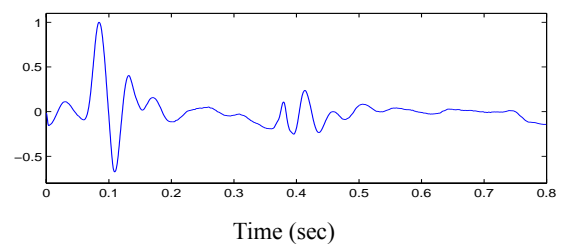


Figure 13 Final PCG heart-beat signal.

5 Conclusions

In this article a method was described which decomposes the PCG signal into its constituent heart-beat cycles using the ECG signal. Five algorithms have been devised to carry out this task. These algorithms are summarized in TABLE 2.

TABLE 2 – Algorithms used to decompose the PCG signal and reconstruction of an artefact-free heart-beat signal.

- | |
|--|
| <ol style="list-style-type: none">1) QRS peak detector.2) QRS interval detector.3) ECG beat cycle detector.4) PCG beat cycle detector.5) Heart-beat signal reconstruction algorithm. |
|--|

First the QRS peaks are detected in the ECG signal, then the false peaks are identified and removed using the true QRS interval detector. The third algorithm is used to isolate the cardiac cycles from the ECG signal. This is done by detecting the peak of the P-wave as the beginning of the cardiac cycle. The starting points of the cardiac cycles are then used to decompose the PCG signal into beat-cycles. A template signal is formed from the PCG beat cycles. The correlation coefficients of the template signal with the individual beat cycles are used to identify the artefact free heart-beat cycles. Using frequency domain averaging, the mean of the heart-beat cycles is found and converted back to the time domain as the final heart-beat signal. These algorithms were successfully applied to real signals recorded from patients suspected with coronary artery disease.

REFERENCES

- [1] Rushmer, R. F., 1970, "Cardiovascular dynamics," W. B. Sanders Company, Philadelphia, PA.
- [2] Akay, M., Welkowitz, W., Semmlow, J. L., et al., 1991, Med & Biol. Eng. & Computing, **29**, 365-372.
- [3] Tinati, M. A., Bouzerdoum, A, Mazumdar, J., and Mahar, L., 1997, "Time-Frequency analysis of heart sounds before and after angioplasty", Proc. IEEE Int. Conf. on Digital Signal Processing (DSP' 97), 75-79, July, 1997, Santori Greece.
- [4] Tinati, M. A., Bouzerdoum, A, Mazumdar, J., and Mahar, L., 1998, "Short time Fourier analysis of phonocardiograms before and after angioplasty", Proc. of Third Biennial Eng. Math. and Application Conf., (EMAC' 98), 495-498, July 1998, Adelaide Australia.
- [5] Benetley, P. M., Grant, P. M., and McDonnell, J. T. E., 1998, IEEE Trans. Biomed. Eng., **45**, 125-128.
- [6] Friensen, G. M., Jannett, T. C., Jadallah, M. A., et. al., 1990, IEEE Trans. Biomed. Eng., **37**, pp. 85-98.
- [7] Wood, J. C., and Barry, D. T., 1994, Med. Biol. Eng. Comput., **32**, S71-S78.
- [8] Zhang, X., Durand, L.-G., et. al, 1998, IEEE Trans. Biomed. Eng., **45**, 972-979.